Structural Rearrangements of Tubulin and Actin during the Cell Cycle of the Yeast *Saccharomyces*

J. V. KILMARTIN and A. E. M. ADAMS*
*Medical Research Council Laboratory of Molecular Biology, Cambridge CB2 2QH, England; and *Division of Biological Sciences, University of Michigan, Ann Arbor Michigan 48109*

ABSTRACT The distribution of actin and tubulin during the cell cycle of the budding yeast *Saccharomyces* was mapped by immunofluorescence using fixed cells from which the walls had been removed by digestion. The intranuclear mitotic spindle was shown clearly by staining with a monoclonal antitubulin; the presence of extensive bundles of cytoplasmic microtubules is reported. In cells containing short spindles still entirely within the mother cells, one of the bundles of cytoplasmic microtubules nearly always extended to (or into) the bud. Two independent reagents (anti-yeast actin and fluorescent phalloidin) revealed an unusual distribution of actin: it was present as a set of cortical dots or patches and also as distinct fibers that were presumably bundles of actin filaments. Double labeling showed that at no stage in the cell cycle do the distributions of actin and tubulin coincide for any significant length, and, in particular, that the mitotic spindle did not stain detectably for actin. However, both microtubule and actin staining patterns change in a characteristic way during the cell cycle. In particular, the actin dots clustered in rings about the bases of very small buds and at the sites on unbudded cells at which bud emergence was apparently imminent. Later in the budding cycle, the actin dots were present largely in the buds and, in many strains, primarily at the tips of these buds. At about the time of cytokinesis the actin dots clustered in the neck region between the separating cells. These aspects of actin distribution suggest that it may have a role in the localized deposition of new cell wall material.

Actin and tubulin are major structural proteins in all eucaryote cells. They form distinct filamentous structures in the interphase cytoskeleton and during mitosis, also they may be involved in many motile events in eucaryotes. However, in nonmuscle cells only a few of their functions such as the role of actin in cytokinesis (52) and tubulin in flagellar movement (19) are reasonably well established. Their role in other cellular motility events such as intracellular movement of organelles or chromosome movement is as yet unclear. A genetic analysis of these problems might illuminate the precise functions of actin, of tubulin and, in particular, of proteins associated with them. For this purpose, yeast, as a genetically tractable eucaryote microorganism possessing tubulin and actin closely similar to those of higher organisms (21, 30, 36, 60), may be of great value. The genes for yeast actin (18, 44, 53) and tubulin (43) are already under intensive study and most cloned yeast genes can now be mutagenized in vitro and substituted for the wild-type gene in the correct chromosomal position (51). Moreover studies of "pseudorevertants" of such mutants can be expected to yield much information about protein interactions (6).

It is therefore of considerable interest to investigate the distribution of actin and tubulin during the cell cycle in yeast. The arrangement of microtubules in yeasts has been well studied by electron microscopy (8–10, 32, 40, 41, 46, 49) and shows a spindle resembling those of higher eucaryotes as well as cytoplasmic or astral microtubules. Centrioles are not present, but specialized areas of the nuclear envelope (which remains intact during division) function as spindle poles and as an apparent organizing center for the cytoplasmic microtubules. Nothing is known of the arrangement of actin filaments in yeasts, apart from a preliminary indication of their presence by electron microscopy in *Schizosaccharomyces pombe* (56), though more extensive studies of the arrangements of microfilaments have been made in other fungi (20, 26).

This paper describes the application to yeast of immunofluorescence methods. Since these methods permit the exami-

THE JOURNAL OF CELL BIOLOGY · VOLUME 98 MARCH 1984 922-933
 · 0021-9525/84/03/0922/12 $1.00

nation of large numbers of cells, they are of great value in piecing together the behavior of proteins of interest during the successive stages of the cell cycle. Previous studies of yeast internal structures by immunofluorescence employed spheroplasts or isolated cell fractions (31). Here we adapted the procedure to cells that were first fixed and then stripped of their cell walls by enzymatic digestion. This resulted in good preservation of the overall shape and spatial relationships of the cell and allowed morphogenetic events in the cytoplasm to be related to those in the cell wall. In addition, the position of a particular cell in the cell cycle can be determined approximately by comparison of mother and bud cell lengths (10, 47, 62).

A monoclonal antitubulin YOL1/34 (31) and an affinity purified polyclonal anti-yeast actin were used either singly, or together in double labeling experiments. Antitubulin staining was also combined with tetramethylrhodaminyl phalloidin (Rh-phalloidin),[1] a specific fluorochrome for F-actin (16, 64). The distribution of actin showed novel and interesting features, including a ring of F-actin containing dots at the site of bud formation. Double labeling of cells with intact walls with both Rh-phalloidin and the polysaccharide specific dye Calcofluor (54) showed the ring of actin dots was coincident with the newly deposited chitin ring that is laid down at the site of bud formation. This and the changes in the pattern of staining of the actin dots during the cell cycle suggest a possible function for actin in cell wall growth in yeast.

MATERIALS AND METHODS

Yeast Strains and Culture Conditions: Most experiments were performed with *Saccharomyces uvarum* NCYC 74, cultured as described previously (30). Other experiments were performed with *Saccharomyces cerevisiae* strains A364A (23), DC113 (55), Y55 (39), C276 (1), NCYC 366, and NCYC 661 (the last two strains were obtained from the National Collection of Yeast Cultures, Nutfield, England). Strains DC113 and NCYC 366 were cultured similarly to *S. uvarum*, strains A364A, Y55, and NCYC 661 were cultured in YPD (2% glucose, 2% bactopeptone, 1% yeast extract, 40 μg/ml adenine, and 40 μg/ml uracil), and strain C276 was cultured as described in the accompanying paper (1).

Preparation of Yeast Actin: Yeast actin was prepared by the method of Zechel (65). Samples of DNase I (DN-CS, Sigma Chemical Co., Poole, England) were analysed by SDS 12% PAGE (37) to check for proteolytic degradation. Those with <20% degradation were coupled to CNBr activated Sepharose 4B (Pharmacia Fine Chemicals, Hounslow, England) as instructed by Pharmacia but in the presence of 0.1 mM $CaCl_2$. Yeast (*S. uvarum* NCYC 74) cell lysate (30) was processed as described by Zechel (65). The yield was 3 mg actin/50 g (wet weight) cells. The capacity of the DNase I-Sepharose column was consistently only 10% of that expected on a binding ratio of 1 mol actin/mol DNase I.

Preparation and Assay of Antisera: 50 μg of yeast actin was emulsified in Freunds complete adjuvant and injected intraperitoneally into four AO/LOU rats. Boosts in incomplete adjuvant were given at week 3, 7, 12 and 17. At week 4, three rats were giving antiactin detectable in a dot blot assay of the serum at dilutions of 1:1,000. The dot blot assay was a modification of the nitrocellulose spot assay (17); instead of binding antigen to the whole of the nitrocellulose sheet, 1 μl of 200 μg/ml yeast actin was spotted onto the sheet at intervals of 1 cm marked by pencil dots. After blocking the nitrocellulose with blot buffer (0.05 M Tris-HCl, pH 7.5, 0.15 M NaCl, 0.05% Nonidet P-40, 5 mM EDTA, 0.25% gelatin, 0.02% NaN_3), it was blotted with paper tissue and air dried. 1-μl samples of diluted serum were applied to the antigen spots and air dried (17). After washing in blot buffer containing 0.5% Nonidet P-40 and 0.1% SDS, the nitrocellulose sheet was incubated with 10^6 cpm ^{125}I-anti-rat IgG/ml for 60 min at 22°C. The anti-rat IgG (Miles Laboratories, Slough, England) was affinity purified using rat monoclonal YL1/2 IgG coupled to Sepharose 4B as absorbant (31) and then coupled to ^{125}I. After washing as above the nitrocellulose sheet was exposed to x-ray film at −70°C. At week 19 the rats were bled weekly from the tail to give 0.5 to 1.0 ml serum per bleed: these samples of serum were used for all the experiments described in this paper.

The sera were affinity purified using yeast actin coupled to Sepharose as absorbant. 1 mg of yeast actin was gel filtered by centrifugation (42) against 2 mM triethylamine-HCl, pH 7.5, 10 μM ATP, 0.2 mM $CaCl_2$, 0.1 mM dithiothreitol and coupled to 1 g CNBr-Sepharose 4B as instructed by Pharmacia. A 0.5 ml column of actin-Sepharose was equilibrated with 0.05 M potassium phosphate, pH 7.4, 0.15 M NaCl (PBS) and 0.3 ml antiserum passed through the column at 22°C. The antiactin was eluted in 0.5 ml fractions at 4°C with 0.2 M glycine-HCl pH 2.5 and immediately neutralised with 3 M Tris. Usually the first fraction, which before dilution was 200 μg/ml, was diluted 1:100 in the experiments described here, though the later fractions also had usable antiactin.

The specificity of the antisera were shown by staining of nitrocellulose blots of 10% SDS polyacrylamide gels (59). Yeast cells were broken by glass beads and immediately boiled in two times concentrated SDS gel sample buffer (37). The viscosity was reduced by sonication and cell walls removed by centrifugation. This extract was separated on a 10% SDS polyacrylamide gel using wide sample slots and proteins were electrophoretically transferred to nitrocellulose (59). After blocking the nitrocellulose transfers with blot buffer (see above), strips 2–3 mm wide were cut, blotted with tissue paper and air dried. 100 μl of 2 μg/ml monoclonal antitubulin YOL1/34 or of a 1:100 dilution of affinity purified antiactin were added to each dry strip so that it was uniformly moist and the strip was then allowed to air dry. The strips were washed and reacted with ^{125}I-anti-rat IgG as described for dot blots above.

The antiactin was coupled to fluorescein isothiocyanate (FITC) by first precipitating the antibodies from serum with 50% $(NH_4)_2SO_4$, gel filtering against 0.25 M $NaHCO_3$-0.025 M $NaCO_3$ (pH 8.9), and reacting with 0.05 mg FITC/mg protein at 4°C overnight. The FITC-conjugated antibodies were affinity purified as described above.

Fixation and Immunofluorescence of Yeast Cells: Asynchronous early log phase yeast cells were fixed by several methods. Either (*a*) cells were harvested by filtration (1.2 μm filters) and immediately washed and resuspended in 0.1 M potassium phosphate buffer, pH 6.5, containing fixative, or (*b*) fixative was added directly to the cells growing in medium followed by buffer to give a final pH of 6.5 and, after 30 min at 25°C, the fixed cells were harvested and resuspended as in the first procedure. Fixation was for a total of 90 min at 25°C and employed either 3.7% formaldehyde or 3% paraformaldehyde plus 1% glutaraldehyde ($OD_{235}/OD_{280} < 0.20$). The paraformaldehyde was always added before the glutaraldehyde. Fixatives were removed by washing three times with 0.1 M phosphate, pH 6.5, and once with 1.2 M sorbitol in 0.12 M K_2HPO_4/0.033 M citric acid (pH 5.9). The formaldehyde fixed cells were digested with 1/10 volume snail gut juice (Helix pomatia juice, Uniscience, Cambridge, England) and 1/100 volume 50 mg/ml Zymolyase 5000 (Miles Laboratories). The paraformaldehyde/glutaraldehyde fixed cells had in addition 1/400 volume Mutanase (Novo Enzymes, Windsor, England). The presence of sorbitol was not essential, but was added for extra protection of the cells. After digestion for 90 min at 30°C, the cells were washed with sorbitol containing buffer and applied to polylysine coated multiwell slides (31), and fixed for 6 min in methanol and 30 s in acetone both at −20°C. The paraformaldehyde/glutaraldehyde fixed cells were then given three 5-min treatments with fresh 1 mg/ml $NaBH_4$ in PBS. Experiments with *S. cerevisiae* strain C276 employed the alternative fixation and permeabilization procedures described in the accompanying paper (1).

Monoclonal antitubulin YOL1/34 IgG (31) or affinity purified antiactin was added after dilution in bovine serum albumin (BSA)-PBS (31), YOL1/34 IgG was 20 μg/ml and antiactin was diluted 1:100 (to 2 μg/ml). After washing with BSA-PBS, affinity purified FITC anti-rat IgG (31) was added, usually at a dilution of 1:10 in BSA-PBS. For formaldehyde fixed cells, the incubations were 1–3 h at 22°C, for paraformaldehyde/glutaraldehyde fixed cells they were 7–12 h at 37°C. For double antibody labeling, the cells were reacted with YOL1/34 and affinity-purified rhodamine-coupled anti-rat IgG as above. Surplus rat IgG binding sites were blocked with 1 mg/ml rat IgG (28) for 30 min at 22°C, then undiluted affinity purified FITC rat antiactin was applied for 10 h at 37°C.

For double labeling with Rh-phalloidin and antiactin, formaldehyde-fixed cells in 1.2 M sorbitol/0.12 M phosphate-citrate, pH 5.9, containing 1% (vol/vol) Triton X-100 were treated with 20 μg/ml Rh-phalloidin for 2 min at 22°C. These cells were applied to a polylysine coated slide and fixed in acetone at −20°C for 3 min. They were then stained with undiluted affinity-purified antiactin for 8 min at 22°C and washed with PBS. Undiluted affinity purified FITC anti-rat IgG was then added for 8 min at 22°C followed by washing in PBS.

For double labeling with Rh-phalloidin and antitubulin, the Rh-phalloidin

[1] *Abbreviations used in this paper:* Rh-phalloidin, tetramethylrhodaminyl phalloidin; BSA, bovine serum albumin; FITC, fluorescein isothiocyanate; DAPI, 4′,6-diamidino-2-phenylindole; PBS, 0.05 M potassium phosphate, pH 7.4, 0.15 M NaCl.

treated cells were applied to a polylysine coated slide and washed with PBS containing 2 μg/ml Rh-phalloidin (all buffers subsequently contained 2 μg/ml Rh-phalloidin). YOL1/34 monoclonal antitubulin was added at 200 μg/ml in BSA-PBS for 10 min at 22°C. After washing with PBS, affinity-purified FITC anti-rat IgG diluted with an equal volume of PBS was applied for 10 min at 22°C, followed by washing.

For double labeling with Calcofluor and Rh-phalloidin, formaldehyde-fixed cells whose walls had not been digested were labeled first with Calcofluor White M2R (54) and, after washing, with 20 μg/ml Rh-phalloidin in PBS containing 1% (vol/vol) Triton X-100 for 2 min at 22°C.

Cells were also labeled with Rh-phalloidin after fixation in 70% ethanol 4 mM EGTA, pH 6.2. Log phase cells in media were added to 95% ethanol, 5 mM EGTA, pH 6.2, at −20°C to give the final concentrations indicated and were allowed to warm to 4°C. After 5 min at 4°C cells were pelleted, resuspended in 70% ethanol, 4 mM EGTA pH 6.2 and incubated with 20 μg/ml Rh-phalloidin and 1% (vol/vol) Triton X-100 for 2 min at 4°C.

All slides were mounted in p-phenylenediamine/90% glycerol (29) containing 0.05 μg/ml 4′,6-diamidino-2-phenylindole (DAPI) (63). Slides were photographed using the chromogenic black and white film Ilford XP1 400 ASA, on a Zeiss standard WL microscope equipped for epifluorescence with a HBO 50W high pressure mercury lamp. A Zeiss planachromat 100X N.A. 1.25 or Neofluor 100X N.A. 1.3 objective was used with Zeiss selective FITC (487710) and rhodamine (487715) filters. For phase-contrast and DAPI staining a Ph3 Neofluor 100X N.A. 1.3 objective and for Calcofluor staining a Neofluor 100X N.A. 1.3 objective was used, both with Zeiss UV filters (487701).

RESULTS

Purification of Yeast Actin

Yeast actin was purified by affinity chromatography on DNase I-Sepharose (Fig. 1, lane *2*) using the elution protocol of Zechel (65), which uses a formamide eluant to minimise denaturation. On addition of 2 mM $MgCl_2$, 80–90% of the actin became sedimentable as filaments of 7–8-nm diameter (Fig. 2). The assembly characteristics of yeast actin prepared by this procedure were not investigated in detail as this was not necessary for the preparation of antisera.

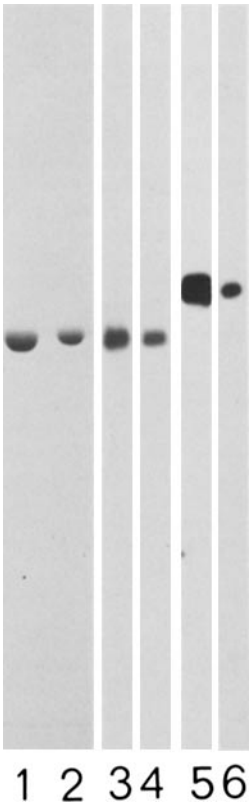

FIGURE 1 Purification of yeast actin and characterization of the specificity of the antiactin and antitubulin antibodies. (Lanes *1* and *2*) 10% SDS polyacrylamide gels (37) of muscle (lane *1*) and yeast (lane *2*) actin stained with Coomassie Blue. (Lanes 3–6) Nitrocellulose blots of 10% SDS polyacrylamide gels containing purified yeast actin (lane *3*), whole yeast cell extract (lanes *4* and *6*), or purified yeast tubulin (lane *5*). Lanes *3* and *4* were stained with affinity purified antiactin and ^{125}I-labeled anti-rat IgG, lanes *5* and *6* with monoclonal antitubulin YOL1/34 and ^{125}I-labeled anti-rat IgG (see Materials and Methods).

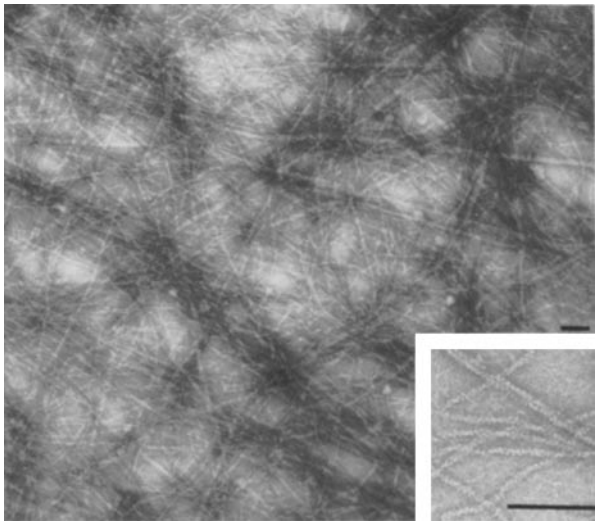

FIGURE 2 Yeast actin filaments polymerised by addition of 2 mM $MgCl_2$ negatively stained with 1% uranyl acetate. Bar, 100 nm. × 40,000. (*Inset*) Bar, 100 nm, × 120,000.

Specificity of the Antibodies

The antiactin antibodies were produced in rats and affinity-purified before use. When applied to nitrocellulose blots of whole yeast cell proteins separated by SDS PAGE, they stained a single band with the same mobility as that of purified yeast actin (Fig. 1, lanes *3* and *4*). Antibodies from two individual rats were used for most of the experiments in this paper with very similar results. Affinity-purified antibodies from one of these rats, when used to stain mouse 3T3 tissue culture cells (31), gave the usual actin stress fiber staining pattern (3; data not shown), though higher concentrations of antibody were required (70 μg/ml) compared with the 2 μg/ml normally needed for antiactin immunofluorescence in yeast.

The monoclonal antitubulin antibody YOL1/34 binds strongly to yeast tubulin in a solid phase immunoassay (31) and is specific for a band with similar mobility to that of purified yeast tubulin (30) when applied to nitrocellulose blots of whole yeast cell proteins (Fig. 1, lanes *5* and *6*). In *Physarum* YOL1/34 recognises α-tubulin specifically (14); it has not been established whether the same subunit is recognised in yeast.

Antitubulin Immunofluorescence of Yeast Cells

S. uvarum and *S. cerevisiae* cells stained with monoclonal antitubulin YOL1/34 and FITC anti-rat IgG are shown in Fig. 3, *a* and *c*, together with the corresponding combined DAPI fluorescence (for DNA staining reference 63) and phase-contrast (Fig. 3*b*) or bright-field view (Fig. 3*d*). The results obtained are in good agreement with the electron microscopic results (8) and are summarized in diagrammatic form in Fig. 10. In particular: (*a*) Virtually every yeast cell shows antitubulin staining, in agreement with the finding that spindle pole bodies have intranuclear microtubules throughout the cell cycle (9). The staining of intranuclear microtubules always runs through the region of the nucleus occupied by nuclear DNA as revealed by DAPI staining. (*b*) In cells with small buds that have apparently not yet formed complete spindles (Fig. 3*a*, cell 1; Fig. 3*c*, cell 1; see also Fig. 10, *b* and

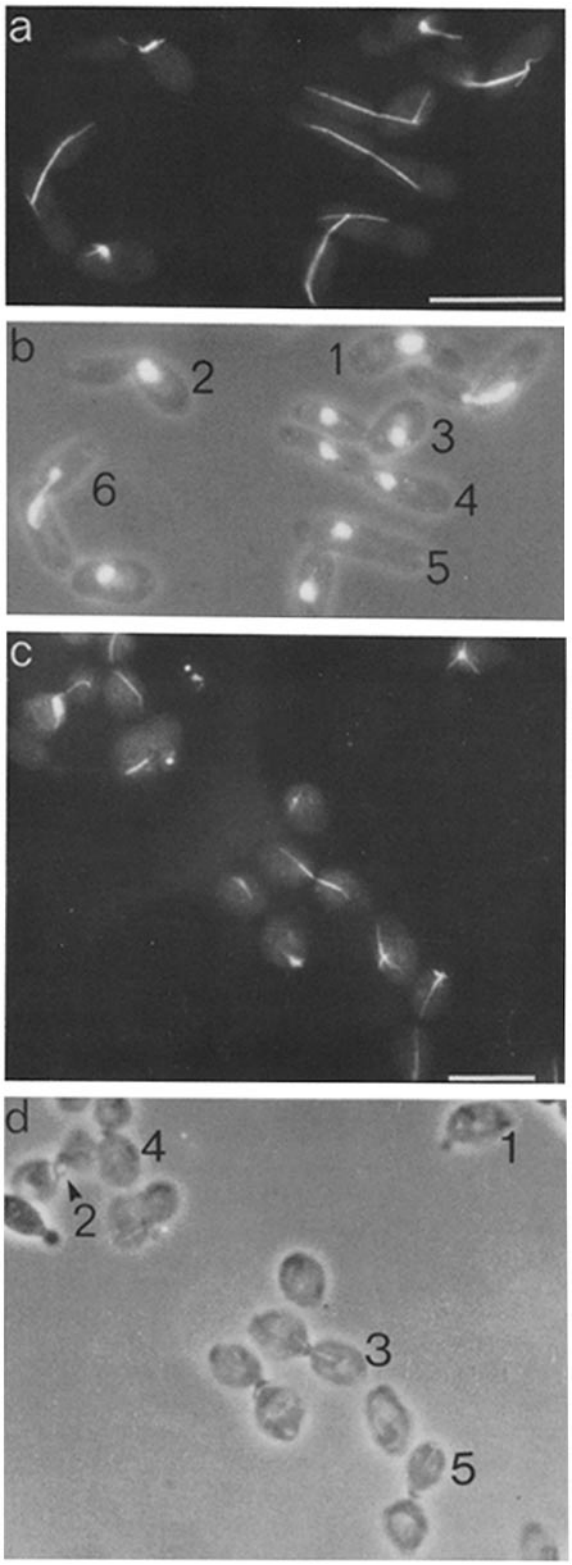

FIGURE 3 Microtubule localization in budding yeast cells. (*a* and *b*) Indirect immunofluorescence with monoclonal antitubulin YOL1/34 (*a*) and phase-contrast plus DAPI fluorescence (*b*) views of *S. uvarum* cells fixed with 3% paraformaldehyde/1% glutaraldehyde, methanol, and acetone, and stained as described in Materials and Methods. (*c* and *d*) Indirect immunofluorescence with monoclonal antitubulin YOL1/34 (*c*) and bright-field (*d*) views of *S. cerevisiae* (strain C276) cells prepared by procedure 2 of the accompanying manuscript (1). (Note that microtubule fluorescence is dimly visible in Fig. 3*d* because the ultraviolet illumination was continued during the bright-field photography.) Similar cytoplasmic and spindle microtubules were seen (data not shown) in the other strains of *S. cerevisiae* examined (A364A, DC113, Y55, NCYC 366, and NCYC 661). Bars, 10 μm. (*a* and *b*) × 1,770. (*c* and *d*) × 1,170.

c) cytoplasmic microtubules generally extend to or into the buds (9, 10), although sometimes additional microtubules remain within the mother cells (Fig. 3*c*, cell 1; see also Fig. 6*b*). (*c*) In cells with larger buds short spindles are often found (Fig. 3*a*, cell 2; Fig. 3*c*, cell 2; see also Figs. 6*f*, 8*f*, and 10*d*), these spindles frequently have a "dumbbell" shape. The brighter ends probably correspond to a mixture of the short chromosomal microtubules and the pole to pole microtubules observed by Peterson and Ris (46); the less bright area between the ends would correspond to the pole to pole microtubules only. (*d*) In cells with buds approaching the size of the mother cell (Fig. 3*a*, cells 3–6; Fig. 3*c*, cells 3–5; see also Fig. 10*e*) long spindles are usually found. In *S. uvarum*, these longer spindles were always associated with partially or fully separated chromosomes (judging from the DAPI staining of DNA), depending on their lengths. A proportion of the long spindles appeared dimmer in their mid-regions (Fig. 3*c*, cell 5; see also Fig. 6*k*) presumably because of a decrease in microtubule number in the mid-regions as the spindles break down (see Fig. 10*f*). These spindles were not significantly longer than the fully elongated spindles that had apparently uniform antitubulin staining throughout their length (Fig. 3*a*, cell 3; Fig. 3*c*, cell 4; Fig. 6, *h–j*). There may be a decrease in the apparent intensity of fluorescence per unit length between short and long spindles (35). Unfortunately the complete outlines of the nuclei were not revealed by either phase-contrast or DAPI staining in these cells. However, we presume that the DAPI-stained regions are still connected by long isthmuses of nuclear envelope (Fig. 10, *e* and *f*) so that the pole to pole microtubules remain intranuclear throughout the cell cycle (8, 40, 41).

Two findings from these immunofluorescence studies add significantly to the picture of microtubule distribution obtained previously from electron microscopy. First, prominent and often long bundles of microtubules generally extend beyond both poles of both short and elongating spindles (Fig. 3*a*, cells 2–6; Fig. 3*c*, cells 2–4; Fig. 6, *f–j*, Fig. 8, *f–i*). In *S. uvarum*, the speed of fixation was critical in the preservation of these cytoplasmic microtubules; they were reduced or absent in harvested cells that were left as a concentrated suspension for a few minutes before fixation. Second, in cells with short and medium length spindles that were still entirely within the mother cells, almost always one of the bundles of cytoplasmic microtubules extended to or into the bud (Fig. 3*a*, cell 2; Fig. 3*c*, cell 2; Fig. 6, *e* and *g*; Fig. 8*f*). Of 126 *S. cerevisiae* cells (strain C276) with spindles in this category, 104 clearly had this arrangement of cytoplasmic microtubules, 18 probably did, three were questionable, and one probably did not. Thus the spatial relationship between cytoplasmic microtubules and the budding site that is established earlier in the cell cycle (point *b*, above, and references 8–10) appears to be maintained until the spindle itself migrates to span the neck region connecting the mother cell to its bud. Of the 126 *S. cerevisiae* cells counted, about half had the cytoplasmic microtubules clearly extending beyond the necks into the buds, but in only three of these were microtubules visible all the way to the tips of the buds.

Similar cytoplasmic and spindle microtubule morphologies

were seen in the other strains of *S. cerevisiae* examined (A364A, DC113, Y55, NCYC 366 and NCYC 661). However, a proportion of the *S. cerevisiae* NCYC 366 and NCYC 661 cells examined were impermeable to antibody. *S. uvarum* was used mainly in this paper because it gave the clearest immunofluorescence staining patterns, particularly in double labeling. This is probably because it has a cylindrical growth form and thus combines reasonable size with relative thinness.

Satisfactory visualization of spindle and cytoplasmic microtubules was achieved with a variety of protocols for fixation and permeabilization (compare Figs. 3, *a* and *c*, 6, and 8; see also reference 1). In particular, the methanol and acetone steps appeared dispensable after formaldehyde fixation (see Fig. 8). Fixation with glutaraldehyde without paraformaldehyde considerably reduced the permeability of the cells to antibodies. Also, an alteration in spindle morphology occurred if fixation protocols involving pre-treatment of the unfixed cells with thiols (34, 35, 45) were followed: the rod-like elongated spindles lost microtubules from the mid regions of the spindles and developed thick ends as seen in disintegrating spindles (Fig. 3*c*, cell 5; see also Figs. 6*k* and 8*j*).

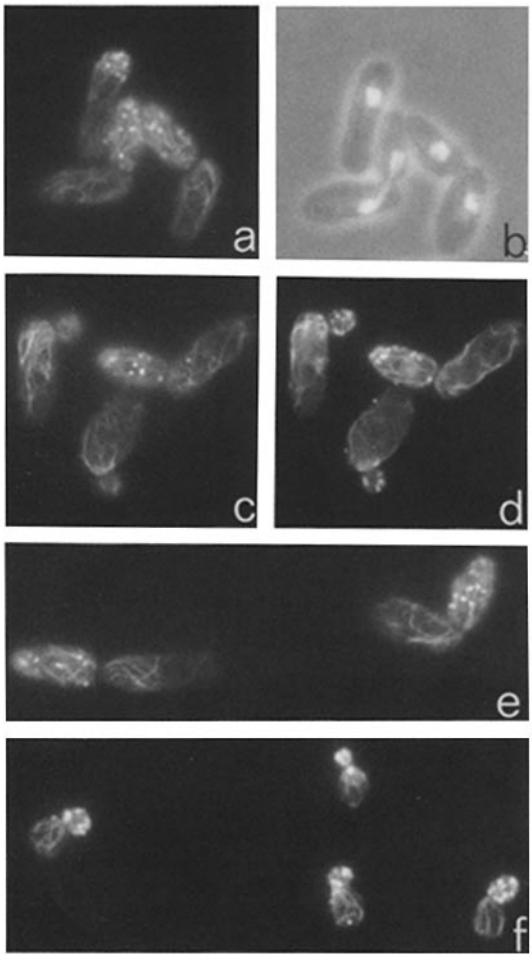

FIGURE 4 Actin localization in budding yeast cells as visualized by indirect immunofluorescence. Cells were stained with affinity-purified rat anti-yeast actin and FITC anti-rat IgG after fixation with 3% paraformaldehyde/1% glutaraldehyde, methanol, and acetone (see Materials and Methods). (*a–e*) *S. uvarum* cells. (*a* and *b*) Immunofluorescence (*a*) and phase-contrast plus DAPI-fluorescence (*b*) views of the same cells; note the mitotic cell in the lower left. (*c* and *d*) Immunofluorescence viewed at different focal planes in the same cells: near the tops of the cells (*c*) and near their middles (*d*). (*e*) Immunofluorescence showing apparent coincidence of staining between dots and fibers. (*f*) Immunofluorescence of *S. cerevisiae* strain A364A. × 1,450.

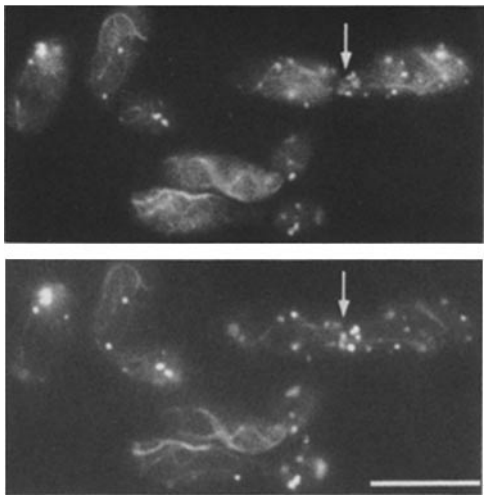

FIGURE 5 Comparison of antiactin immunofluorescence (*top*) and Rh-phalloidin (*bottom*) staining patterns of the same *S. uvarum* cells fixed in formaldehyde and acetone (see Materials and Methods). Bar, 10 μm. × 1,470.

Antiactin Immunofluorescence of Yeast Cells

Some fields of yeast cells fixed in paraformaldehyde/glutaraldehyde, methanol and acetone, then stained indirectly with affinity-purified antiactin antibody and FITC anti-rat IgG, are shown in Fig. 4. The pattern of staining consists of dots and an intricate array of fibers of varying thickness. The dots appear to be more concentrated in the bud or daughter cell, and focussing experiments suggest that the fibers and dots (especially the latter) are concentrated more in the cortex of the cell (Fig. 4*c* and *d*). Occasionally there is overlapping of fluorescence from dots and fibers which might suggest a connection between the two (Fig. 4*e*). Formaldehyde, methanol and acetone fixation of *S. uvarum* also gave similar results (see Fig. 6) and inclusion of 10 mM EGTA was without effect (not shown). Rapid fixation of *S. uvarum* was again essential, otherwise the actin fibers tended to form large bundles. Cell cycle-dependent changes in the pattern of actin staining will be described later.

To confirm the pattern of staining with the antibody, we stained yeast cells simultaneously with antibody and Rh-phalloidin, a reagent specific for F-actin (16, 64), which, like nitrobenzoxadiazole-phallacidin, stains filament bundles and cortical patches in yeast (1, 48). Unfortunately, treatment of Rh-phalloidin stained yeast cells with antiactin caused a rapid dissociation of the Rh-phalloidin from the cells; consequently, antibody treatments had to be rapid with high concentrations of antibody, conditions that are not ideal. Staining with Rh-phalloidin after antibody incubations was unsatisfactory. Despite these problems, there was good agreement between the two reagents (Fig. 5), though there are definite differences in intensity of staining of the dots. Occasionally there are dots stained by only the antibody or only Rh-phalloidin. There were more consistent differences in the neck regions of cells about to divide (Fig. 5, arrows). These differences will be discussed later.

Two negative controls for the antiactin staining were carried out: first, preimmune serum was passed through the actin-Sepharose column and eluted as for the affinity purification of antiactin from the immune serum; second, the affinity-

purified antiactin was absorbed by mixing with actin-Sepharose beads. When the staining protocol was carried out in either case, the features of the antiactin staining were absent though the outline of the cells could be seen dimly. When these images were photographed and printed under identical conditions to Fig. 4, completely featureless black prints were obtained (data not shown).

A different fixation protocol for *S. uvarum*, 70% ethanol and 4 mM EGTA, pH 6.2, followed by staining with Rh-phalloidin in 1% Triton X-100, gave the same type of staining patterns (data not shown). Various other controls on Rh-phalloidin staining itself are presented in the accompanying paper (1).

The strains of *S. cerevisiae* examined, A364A (Fig. 4*f*), DC113, Y55, NCYC 366, and NCYC 661 gave similar antiactin staining to *S. uvarum*, except as noted below.

Double Label Immunofluorescence of Tubulin and Actin in Yeast Cells

Double label immunofluorescence of tubulin and actin was carried out to see whether there was any detectable relationship between microtubule and actin filament localization in yeast cells, and to attempt to relate the patterns of actin localization to stages in the cell cycle. The method used was that of Hynes and Destree (28): yeast cells were stained first with antitubulin YOL1/34 and rhodamine-coupled anti-rat IgG, surplus binding sites for rat IgG were blocked by incubating with excess rat IgG, and affinity-purified FITC-coupled rat antiactin was added. Because the antiactin is just a single antibody layer, it is somewhat dimmer than in Fig. 4. However, this sequence of antibody incubations could not be reversed because staining with FITC-coupled YOL1/34 was too dim to reveal cytoplasmic microtubules. The various combinations of tubulin and actin staining seen in individual log-phase *S. uvarum* cells could be grouped into classes and quantified as illustrated in Figs. 6 and 7 and are described in more detail in the legends to these figures.

The budded cells (Fig. 6) have been placed in order of their approximate sequence in the cell cycle (apart from Fig. 6*f*; see below). The approximate cell cycle position of an individual cell was assessed from a combination of relative bud size (10, 47, 62) and the spindle length (10) as judged from

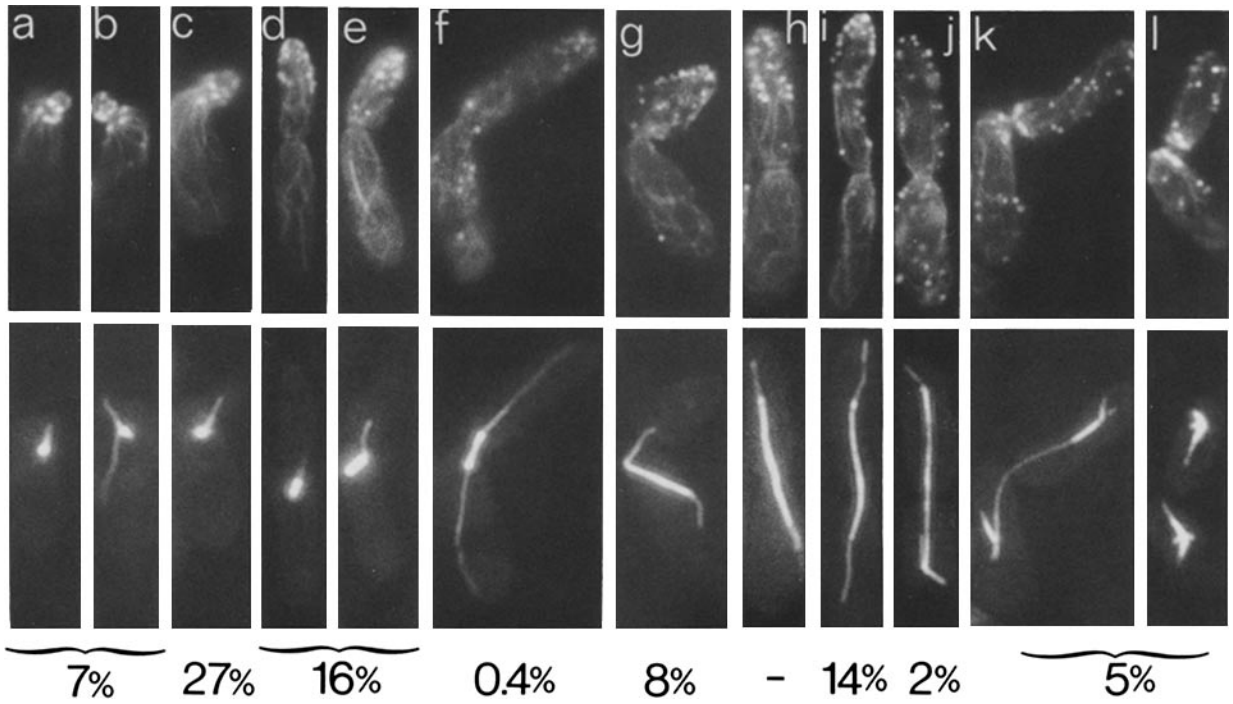

FIGURE 6 Double immunofluorescence of actin (*top* row) and tubulin (*bottom* row) distributions of individual cells during the budding cycle. Log-phase *S. uvarum* cells fixed with formaldehyde, methanol, and acetone were double-labeled for immunofluorescence with affinity-purified antiactin and monoclonal antitubulin YOL1/34 (see Materials and Methods) and photographed in the same focal plane. The representative cells shown here have been placed from left to right in order of increasing spindle length (or bud size where no spindle is present), hence in order of their approximate sequence in the cell cycle. The numbers underneath the micrographs are the percentages of cells with the corresponding combinations of tubulin and actin staining in a log-phase population of 990 cells. (The unbudded cells from this same population are illustrated and tabulated in Fig. 7.) The criteria used to classify the staining patterns were as follows. (*a* and *b*) Cells have small buds and actin dots at the bases of the buds; spindles are not yet formed, so tubulin staining consists of a bright dot plus one or more bundles of cytoplasmic microtubules one of which passes into the bud. (*c*) Cells have larger buds. Tubulin staining is as in *a* and *b*, but there are no actin dots at the bases of the buds and practically all such dots are in the buds. In some cells (typically with relatively large buds), the dots are concentrated at the bud tips. (*d* and *e*) Cells generally have still larger buds, and the principal tubulin staining becomes bar or "dumbbell" shaped, indicating spindle formation. Actin dots remain concentrated in the buds, particularly towards the tip regions. (*f*) Mothers and buds are about equal in size, but the spindles have not yet elongated; long cytoplasmic microtubules are present. (*g*) Spindles are elongating (the DAPI staining is usually rod shaped); the actin dots remain concentrated towards the tips of the buds. (*h* and *i*) The spindles have elongated (the DAPI staining shows two clearly separated foci); the actin dots remain concentrated towards the tips of the buds. (*j*) The spindles are elongated, but the actin dots are now distributed between mothers and buds. (*k* and *l*) The spindles are conspicuously less bright in their mid-regions (*k*) or have apparently disintegrated in this region (*l*); the actin dots remain about equally distributed between mothers and buds, but are usually concentrated in the neck regions. × 2,000.

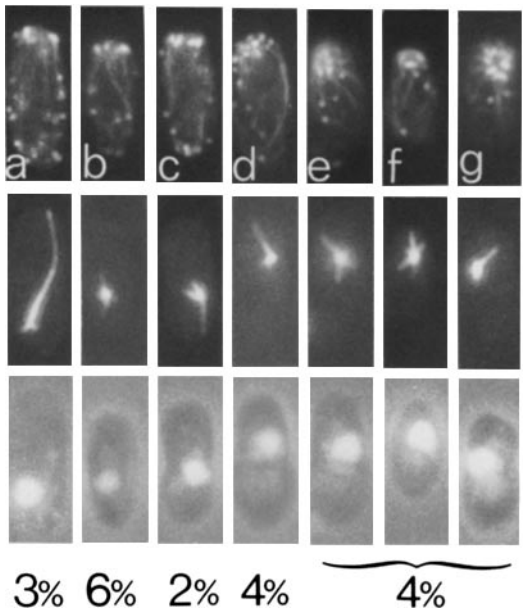

FIGURE 7 Double immunofluorescence of actin (*top* row) and tubulin (*middle* row), together with DNA staining (*bottom* row; DAPI-fluorescence plus phase-contrast), to show distributions in the apparently unbudded cells from the same population as shown in Fig. 6. Cells were prepared and photographed as described for Fig. 6, and the numbers below the photographs have the same meaning as in that figure. The staining patterns were classified as follows. (Note that no temporal sequence is necessarily implied—see text.) (a) Actin dots are found over most of the surface with apparently a concentration at one end; a long, tapering microtubule bundle points towards the concentrated dots. (*b*) Cells have the same actin pattern as in a, but only short microtubules are present. (c) Cells have the same actin pattern as in a, but thin microtubule bundles point to the ends of the cells opposite the concentrated actin dots; there are occasionally slightly higher concentrations of actin dots at these ends of the cells as well. (*d*) Cells have most of the actin dots in a patch, with some microtubules pointing towards them. (e–g) Cells have most of the actin dots in a circle with microtubules pointing towards them. × 2,000.

antitubulin staining. Cells with small buds appear to have a ring or partial ring of actin dots around the base of the bud, with occasionally some dots in the bud (Fig. 6, *a* and *b*; see also Fig. 10*b*), and actin fibers, seemingly connected to the dots, passing into the mother cell. Cytoplasmic microtubules generally point towards or enter the buds, as discussed above in relation to Fig. 3. Cells with larger buds never have actin dots at the bases of their buds; apparently, as the buds grow, the rings of actin dots at their bases disappear and the dots become concentrated in the buds (Fig. 6*c*; Fig. 10*c*). As the buds continue to grow, the actin dots appear to concentrate at their tips (Fig. 6, *d*, *e* and *g–i*; see also Fig. 10*d*). Budded cells without spindles (Fig. 6, *a–c*) were the most abundant class in the population; buds can become quite large before spindle elongation (10). After bud length becomes greater than about half the mother-cell length, the spindle forms (Fig. 6, *d* and *e*) and subsequently elongates (Fig. 6, *g–j*). During spindle elongation most of the cells have similar staining patterns for actin, with dots concentrated in the buds, and especially towards the tips of the buds (Fig. 6, *d*, *e*, and *g–i*), the basal halves of the larger buds and the mother cells have arrays of actin fibers with occasional possible connections to the actin dots (Fig. 6*e*). At later stages of the cell cycle, when cells have large buds and fully elongated spindles, the actin dots appear to distribute more equally between mothers and buds (Fig. 6*j*; see also Fig. 10*e*). Near the end of the cell cycle, when cells have very large buds and long spindles with diminished or disintegrated mid-regions, the actin dots remain equally distributed between mothers and buds, but usually (80% of the cells examined) appear to concentrate in no specific arrangement in the neck regions (Fig. 6, *k* and *l*; Fig. 10*f*). There are some rare exceptions to these combinations of actin and tubulin staining patterns; the cell shown in Fig. 6*f* apparently started mitosis late in the budding cycle, as mother and bud are about the same size. Interestingly, this cell shows the pattern of actin dots normally associated with large buds (*cf.* Fig. 6*j*) rather than that normally associated with short spindles (*cf.* Fig. 6, *d*, *e* and *g*). At no stage of the cell cycle was there any detectable consistent association of actin fibers and microtubules as judged from overlapping of the two staining patterns, although coincident staining could sometimes be seen over very short lengths of microtubules.

Cells that were apparently unbudded (small buds can be difficult to see in these preparations when they are at the upper or lower surfaces of the cells as positioned on the slides) could be grouped into five main classes (Fig. 7). In the cells shown in Fig. 7, *a–c*, the concentrated actin dots at one end have no specific arrangement and actin dots are scattered throughout the rest of the cell. In Fig. 7, *e–g*, the actin dots are arranged in a ring usually at one end and there are many fewer actin dots in the rest of the cell. The temporal sequence of these classes is uncertain. However, comparison of these staining patterns with those observed in budded cells (Fig. 6) suggests that the cells of Fig. 7*a* might be displaying one half of a disintegrating spindle (*cf.* Fig. 6, *k* and *l*; see Fig. 10*g*). Also, the cells of Fig. 7, *e–g*, are probably preparing to bud (*cf.* Fig. 6, *a* and *b*; Fig. 10*a*). Studies on synchronized cells might allow further resolution of these stages.

Similar relationships between tubulin and actin localization were found in budded cells of *S. cerevisiae* strain A364A, but the various cell types were not quantitated. There may be a systematic difference among strains of *S. cerevisiae* in the degree of localization of the actin dots to the buds and to the bud tips in cells with medium-sized buds. Although the concentration of actin dots in small buds is clear in various *S. cerevisiae* strains when examined either by antiactin immunofluorescence (Fig. 4*f*) or Rh-phalloidin staining (Fig. 1, *A* and *B* of the accompanying paper [1]), the concentration of actin dots in larger buds does not appear so extreme or consistent (compare Fig. 4*f* with Fig. 1, *A–C* in reference 1). In *S. cerevisiae* strains with relatively spherical growth forms (A364A, DC113, C276 [Fig. 1, *A–C* of reference 1]), clustering of actin dots at the tips of medium-sized buds, if it occurs at all, appears much less pronounced than in *S. uvarum*. However a *S. cerevisiae* strain with more cylindrical growth form (NCYC 366) when stained with Rh-phalloidin was very similar to *S. uvarum*; in cells with medium sized buds, actin dots were highly concentrated in the buds and were more concentrated towards the tips of those buds.

Double Staining with Rh-phalloidin and Antitubulin

To confirm the patterns of actin and tubulin distribution found by double label immunofluorescence, *S. uvarum* cells were also stained with Rh-phalloidin followed by monoclonal

antitubulin YOL1/34 in the absence of methanol or acetone treatment. The results were substantially similar to those found by double label immunofluorescence. Many cells that are apparently unbudded have a ring of actin dots with actin fibers seemingly attached and cytoplasmic microtubules directed towards the ring (Fig. 8, *a–c*). Cells with small buds have actin dots at the base of the buds as well as usually some dots in the buds (Fig. 8, *d* and *e*). As the buds grow these dots disappear and dots become concentrated in the buds especially towards their tips, with fibers visible in the rest of the mother cell and bud (Fig. 8, *f* and *g*). During this period the spindle forms and elongates.

A difference between the antiactin and Rh-phalloidin staining is seen in the neck regions of cells with elongated spindles where a double bar structure stained by Rh-phalloidin is sometimes present (Fig. 8, *h* and *i*), which might be a pair of rings (Fig. 8 *i*). In *S. uvarum* cells with elongated spindles 31% had this double bar structure, but in 48% there appeared to be a single bar or high density staining and 21% had no bar. These double or single bar structures were not found at other stages of the cell cycle. In Rh-phalloidin stained *S. cerevisiae* strains single bar structures were found in the smaller diploid strains (DC113 and Y55; see also Fig. 1 *A*, cell h, of reference 1) and double bars in the larger hexaploid NCYC 661. The nature of these bar structures is uncertain, as they were not seen clearly by antibody staining. This failure might be due to permeability problems for antibody in the neck region (Fig. 5, arrow) though rarely a thin double (Fig. 6 *h*) or single (Fig. 6 *j*) line was seen in this region. Unfortunately the antiactin treated cells were flatter and more rigidly stuck to the slide surface than the Rh phalloidin-treated cells, so no slightly angled cell was found after antibody staining to demonstrate the ring structure.

Cells with disintegrating spindles (Fig. 8 *j*) have the more equal distribution of actin dots between mother and daughter, with the dots often concentrated in the neck region, as observed with antiactin staining.

Double Staining with Rh-phalloidin and Calcofluor

A ring of chitin, which can be stained selectively with Calcofluor (54), is deposited in the cell walls of yeast cells that are about to bud (24). The staining is less intense for new buds (Fig. 9 *c*, arrow), and appears to become more intense during bud growth; the chitin ring is then left on the mother cell as an intensely staining bud scar after cell separation (Fig. 9 *b*). Experiments with the chitin synthesis inhibitor polyoxin D (12) and with mutants defective in glucosamine synthesis (4) suggest that formation of the chitin ring is not essential for budding. As rings of actin dots were seen in cells with small buds and apparently unbudded cells, it was of interest to see if this ring of actin dots coincided with the chitin ring on the cell walls. Accordingly, fixed yeasts with intact walls were stained with Calcofluor followed by Rh-phalloidin. Fig. 9 shows that the rings of actin dots in apparently unbudded and small budded cells of *S. uvarum* and *S. cerevisiae* correspond in position with weakly staining chitin rings. Occasionally the corresponding chitin rings are barely discernible (Fig. 9 *d*, arrowhead), and were quite undetectable in some budded

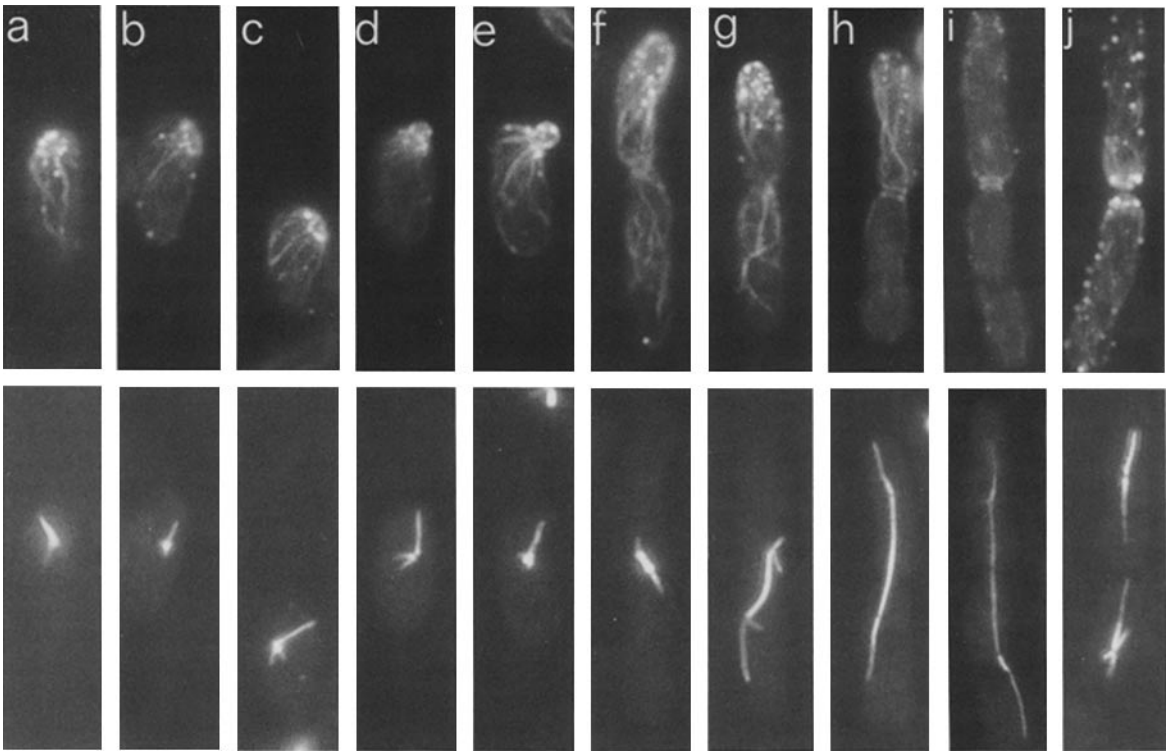

FIGURE 8 Comparison of Rh-phalloidin staining for actin (*top*) and indirect immunofluorescence for tubulin (*bottom*) distributions in individual log-phase *S. uvarum* cells. Cells were fixed with formaldehyde without methanol or acetone treatment and double-stained with Rh-phalloidin (*top* row) and monoclonal antitubulin YOL1/34 plus FITC-anti-rat-IgG (*bottom* row) as described in Materials and Methods. Representative budded (*d–j*) and unbudded (a–c) cells are shown. The former have been ordered from left to right according to spindle length or bud size (cf. Fig. 6). × 1,800.

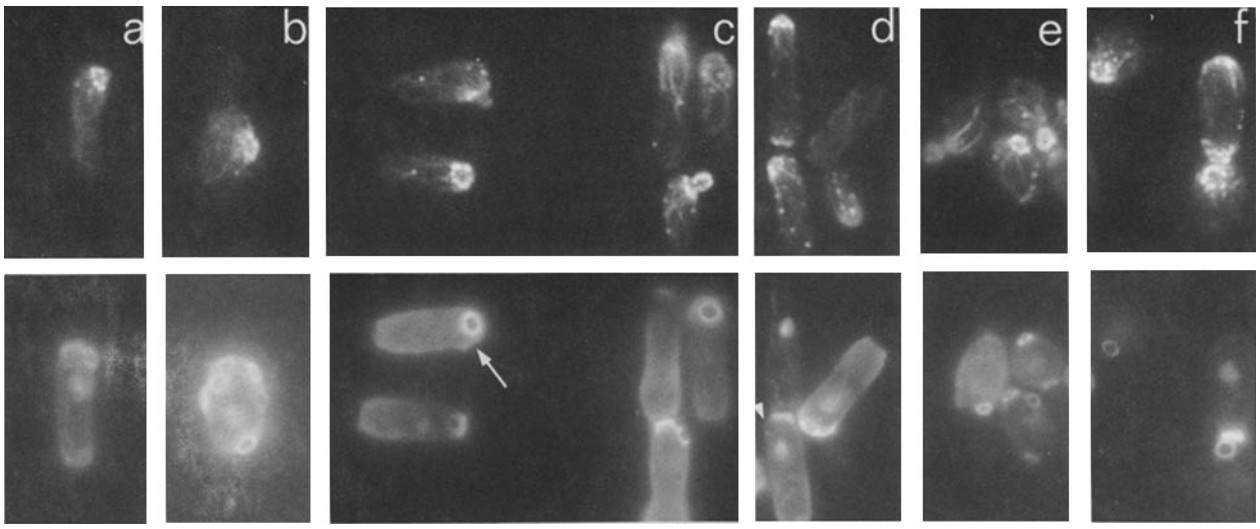

FIGURE 9 Comparison of the distributions of actin (by staining with Rh-phalloidin; top row) and cell-wall chitin (by staining with Calcofluor; bottom row) of formaldehyde-fixed, Triton X-100-treated yeast cells whose cell walls were not digested (see Materials and Methods). (*a–d*) *S. uvarum*. (*e*) *S. cerevisiae* NCYC 366. (*f*) *S. cerevisiae* NCYC 661. The round bodies visible in some of the Calcofluor-stained cells are nuclei, as the mounting medium contained DAPI. × 1,650.

cells (particularly cells with end-on buds; Fig. 9*d*, top). In *S. uvarum*, 75% of apparently unbudded cells that had rings of actin dots had corresponding chitin rings.

DISCUSSION

Purification of Yeast Actin

Yeast actin can be rapidly and easily purified by elution from DNase I-Sepharose with guanidinium hydrochloride, but the product obtained does not readily recover its native properties (60). In contrast, use of a formamide eluant (65) yields a highly purified product (Fig. 1) that polymerizes readily into typical-looking actin filaments (Fig. 2). Although the polymerization and catalytic properties of this actin have not been explored in detail, it is possible that the purification scheme used here will, for certain purposes, be more convenient than the more elaborate schemes used previously for purification of native yeast actin (21, 36).

Immunofluorescence on Whole Yeast Cells

Yeast cells are rather small, rather round, and are encased in a tough and impermeable cell wall. Despite these apparent impediments to effective immunofluorescence, the procedures described here and in the accompanying paper (1) have permitted the effective visualization of intracellular (and even intranuclear) structures in yeast cells whose original shape and spatial relations have been preserved. The procedures are authenticated by the good agreement between immunofluorescence and electron microscopic observations on microtubule localization (see below). The availability of effective immunofluorescence procedures for yeasts should greatly facilitate use of these genetically tractable organisms for study of various problems in cell biology. For example, the clear visualization of both spindle and cytoplasmic microtubules using the monoclonal antitubulin YOL1/34 (31) should facilitate analysis of the phenotypes of mutant yeasts blocked in various steps of the cell cycle (33, 47; *cf.* also Fig. 3 of the accompanying paper [1]).

Microtubule Localization during the Yeast Cell Cycle

As detailed in Results, the cell cycle dependent patterns of microtubule localization observed by immunofluorescence are in good agreement with the results from electon microscopy (8, 46, 49). Moreover, the presence of long rod-like spindles (Fig. 6*i*) that dissociate into rodlets in the daughter nuclei (Fig. 6*l*) had already been deduced by Robinow and Marak (49) using acid fuchsin staining. In one area, the immunofluorescence observations expand our knowledge of microtubule behavior during the cell cycle. Extended bundles of cytoplasmic microtubules have been observed by electron microscopy both in wild-type cells at the double spindle pole body stage (9, 10) and in *cdc31* mutant cells arrested at the restrictive temperature (7; such cells contain an enlarged but unduplicated spindle pole body). In addition, it has been shown that these microtubule bundles run from the spindle-pole body to (or into) the emerging bud (9, 10). However, despite some electron micrographs showing cytoplasmic microtubules of appreciable length in cells with complete spindles (e.g., Fig. 7 of reference 10 or Fig. 3 of reference 35, see also Fig. 6*f*), it has not been clear either if such extended microtubules are routinely present after spindle formation or if these microtubules (if present) remain oriented toward the budding site until the nucleus itself migrates into the mother-bud neck (8, 10, 47). The immunofluorescence results (Figs. 3, 6, and 8, and associated text) show that prominent bundles of cytoplasmic microtubules are indeed normally present at both poles of the spindle and that one of these microtubule bundles normally runs to or into the bud. Such microtubules could ensure that, before elongation, the spindle is optimally positioned between mother and bud so that one pole is always inserted into the bud during elongation. Cytoplasmic or astral microtubules are present in other fungi, and may play a direct role in the separation of daughter nuclei (2).

Actin-containing Structures in Yeast

The observation that some of the actin in a yeast cell is found in a set of cytoplasmic fibers is consistent with observations on many other types of eucaryotic cells. The fibers visualized here are presumably bundles of individual actin filaments, and there may well be additional filaments that are not visualized by the present methods. In contrast, the actin dots observed here in yeast are rather unusual, though they have now also been observed in another fungus, *Uromyces phaseoli*, after Rh-phalloidin staining (27). Concentrations of actin that may be similar have also been observed in tissue culture cells after transformation and in mouse embryos (5, 13, 38). The actin dots are unlikely to be artifacts, because they were found using several different methods of fixation and were detected with two quite different reagents, affinity-purified antiactin antibodies and Rh-phalloidin (see also reference 1). Phalloidin has much higher affinity for F-actin compared to G-actin (61), so the dots may be composed of F-actin. Greer and Schekman (22) have described the reversible formation in vitro of large nonfilamentous particles of yeast actin induced by 0.1 mM $CaCl_2$. It is possible that these correspond to the actin dots seen here in vivo, but the calcium concentration required to induce their formation in vitro is much higher than the range of calcium ion concentrations thought to be present in eucaryotic cells (57). However, it is possible that the formation of the actin particles in vivo could be facilitated by the presence of one or more actin-binding proteins.

As noted in Results, the actin fibers often appear to be connected to dots, but it is impossible to be certain of this interpretation given the depth of field with the optics used here (~0.5 μm).

Hoch and Staples (27) have proposed that the actin dots seen in the fungus *Uromyces phaseoli* after Rh-phalloidin staining correspond to "filosomes," microvesicles coated with filaments mainly 5–6 nm in diameter (26). Whether such filaments are composed of actin might be tested using the antiactin antibodies described here.

Our results suggest that actin is probably not a constituent of the layer of 10-nm diameter filaments that has been shown by electron microscopy (11) to be attached to the cytoplasmic side of the cell membrane in the neck connecting mother cell to bud. This layer of filaments seems to form gradually as the bud emerges, to remain in place throughout the period of bud growth, and to disappear shortly before cytokinesis (11). In contrast, actin appears to be concentrated at the budding site just before and just after bud emergence, and just before and just after cytokinesis, but not during most of the period of bud growth (see Results and further discussion below). Moreover, the 10-nm filaments lie in the middle of the neck region, whereas the rings of actin dots observed in cells with small buds are generally displaced toward the mother-cell side of the neck. Finally, purified yeast actin polymerizes in vitro into filaments (Fig. 2) that are more typical (in both diameter and other appearance) of actin filaments than are the 10-nm filaments observed in vivo. However, we cannot rule out the possibility that actin in the 10-nm filaments is too sparse to be visualized by the present methods or is somehow inaccessible to the probes, and that the diameter and appearance of the filaments in vivo are affected by the co-polymerization of accessory proteins.

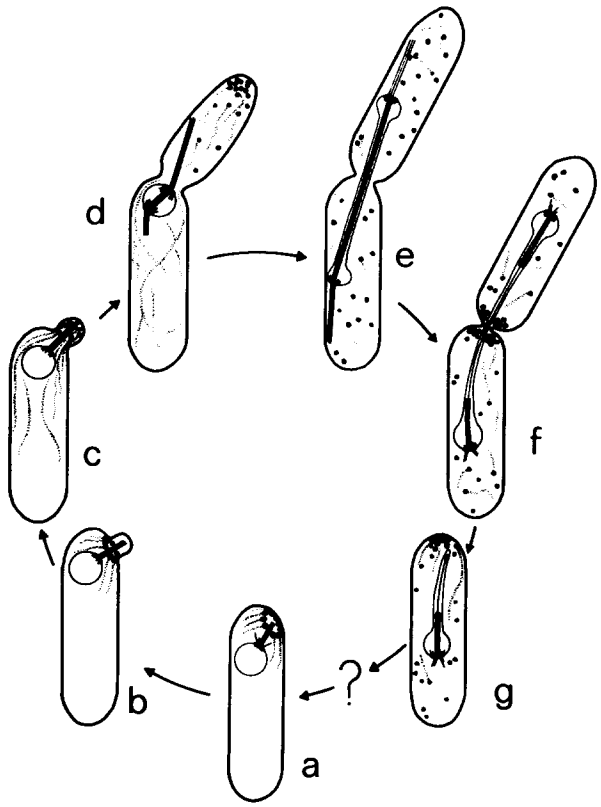

FIGURE 10 Schematic diagram of the changes in actin and tubulin distribution by immunofluorescence during the cell cycle of *S. uvarum*. The nuclei are the round bodies towards the top of cells *a–d* and the elongated bodies of cells *e–g*. Microtubules are represented by straight lines growing from the spindle pole bodies that are the denser areas of the nuclear envelope. Actin is represented by the black dots and actin fibers by dotted lines; the connectivity between dots and filaments ought to be considered tentative (see text). Unbudded cells undergo a series of transitions represented by the question mark; some of these are shown in Fig. 7.

Actin Localization during the Yeast Cell Cycle

The changing patterns of actin localization during the yeast cell cycle (shown schematically for *S. uvarum* in Fig. 10) provide some clues as to the possible function of this protein in yeast. In view of the present uncertainty concerning the role of actin in the spindle (3, 25) it is of particular interest that there was no apparent lengthy direct interaction between actin filaments and microtubules at any stage of the cell cycle (Figs. 6 and 8). However, as it is unlikely that single actin filaments are visible in cells by direct immunofluorescence or Rh-phalloidin labeling, an association of a few actin filaments with either cytoplasmic or spindle microtubules cannot absolutely be excluded.

In contrast to the uncertainty of the role of actin in the mitotic spindle, the changing arrangements of the actin dots during the cell cycle suggest in several ways that actin may be involved in the localized deposition of cell wall materials and in the selective growth of the bud. During the cell cycle the actin dots are specifically associated with the base of small buds, become concentrated in the bud (specifically towards the tip of the bud in some strains), and finally become concentrated in the neck region at about the time of cytokinesis (Figs. 6 and 7). These are all areas of the yeast cell where

active changes in cell wall deposition are occurring (8, 47). The actin dots also appear to be associated with some of the early events in budding. One of these is the deposition of a Calcofluor positive chitin ring (Fig. 9) that precedes the actual emergence of the bud (12, 24, 47). These chitin rings generally appear less bright after Calcofluor staining than do fully formed bud scars (Fig. 9), presumably because of progressive deposition of chitin in the ring during bud emergence. The presence of this weakly staining chitin ring is associated with a corresponding ring of actin dots (Fig. 9). In some apparently unbudded cells with actin dot rings, chitin rings are very faint or absent (Fig. 9 *d*) suggesting that the actin dot ring precedes the deposition of the chitin ring, though this proposal needs confirmation by the use of synchronous cells. In cells with small buds there is a similar ring of actin dots, again coincident with the weakly staining chitin ring (Fig. 9 *c*). In each case the diameter of the actin dot ring is slightly greater than the chitin ring. In both the apparently unbudded cells and the small budded cells with actin dot rings cytoplasmic microtubules have a similar arrangement with microtubules pointing towards the center or side of the ring (Figs. 6, 7, and 8).

It is also possible that the ring of actin dots at the site of bud initiation plays a role in determining the orientation of bundles of actin filaments in the mother cell, as a proportion of these bundles always seems to point towards the bud, even when the bud is lateral (Fig. 4 *c*; see also reference 1). These filament bundles might then be involved in producing a flow of material into the bud by cytoplasmic streaming. The idea that actin might be involved in producing the preferential growth of the cell wall of the bud appears consistent with the observations on the redistribution of actin dots as the bud enlarges. The ring of dots at the base of the bud disappears, but the dots appear concentrated in the bud. In all strains examined, this concentration is pronounced in small buds, though there appears to be strain-to-strain variability in the degree to which the dots are concentrated in larger buds (Figs. 4, 6, 8, and 9; Fig. 1 of reference 1). There also appears to be strain-to-strain variability in the degree to which the dots cluster at the tips of larger buds; this clustering appears to be more pronounced in strains with more elongate growth forms (compare Figs. 6 and 8 here to Figs. 1, 2, and 3 of reference 1). This clustering suggests an involvement of the actin dots in cell wall deposition since cell wall growth is localized in the tip of the bud during at least part of the budding cycle (15, 58; also Fig. 3 of reference 1). As the bud approaches the size of the mother cell, the actin dots redistribute such that they are about equally prevalent in mother and bud (Figs. 6 and 8). As the mother cell wall is not known to be growing during this period, this suggests that the actin dots are not invariably associated with cell-wall growth. This redistribution might be necessary to ensure that later on as the spindle breaks down, there is sufficient actin in both mother and bud to concentrate, as actin dots, on both sides of the neck region (Fig. 6, *k* and *l*). Again, this is a part of the cell undergoing localized cell wall growth as the septum forms and the cells undergo cytokinesis and cell separation.

Labeling of cells with elongated spindles with Rh-phalloidin often revealed a single or double bar structure in the neck region of apparently dividing cells (Fig. 8, *h* and *i*), in appropriately angled cells this appeared ring shaped (Fig. 8 *i*). This structure was only occasionally labeled with antiactin antibodies possibly due to impermeability problems. This structure might be the "microfilamentous septal belt" (20), a ring of microfilaments found by electron microscopy to be present on both sides of the developing septum in two other species of fungi (20, 26). Such a structure has not been found in *S. cerevisiae* after conventional chemical fixation (11), but its presence might be revealed after freeze substitution (26). In *S. cerevisiae*, which has a rather wide septum (11), such a structure, if it were composed of actin filaments, would appear as a double ring structure when stained with Rh-phalloidin at the start of septum formation. This interpretation could be tested by use of the antiactin antibodies described here; impermeability problems might be overcome by postembedding labeling of thin sections (50) with antibodies conjugated to electron-dense markers.

We thank J. Pringle for encouragement, discussion and assistance with the manuscript, Professor Wieland for a generous gift of Rh-phalloidin, J. Fogg for technical assistance, and H. Harris, W. B. Amos, B. M. F. Pearse, M. S. Robinson, and R. A. Crowther for discussion. Thanks are also due to W. B. Amos for Fig. 10.

This work was supported in part by U.S. Public Health Service grant GM-31006 to J. R. Pringle.

Received for publication 21 July 1983, and in revised form 2 November 1983.

REFERENCES

1. Adams, A. E. M., and J. R. Pringle. 1983. Relationship of actin and tubulin distribution to bud growth in wild-type and morphogenetic-mutant *Saccharomyces cerevisiae*. *J. Cell Biol.* 98:934–945.
2. Aist, J. R., and H. W. Berns. 1981. Mechanics of chromosome separation during mitosis in Fusarium (*Fungi imperfecti*): new evidence from ultrastructural and laser microbeam experiments. *J. Cell Biol.* 91:446–458.
3. Aubin, J. E. 1981. Immunofluorescence studies of cytoskeletal proteins during cell division. *In* Mitosis/Cytokinesis. A. M. Zimmerman and A. Forer, editors. Academic Press, Inc., New York. 211–244.
4. Ballou, C. E., S. K. Maitra, J. W. Walker, and W. L. Whelan. 1977. Developmental defects associated with glucosamine auxotrophy in *Saccharomyces cerevisiae*. *Proc. Natl. Acad. Sci. USA.* 74:4351–4355.
5. Boschek, C. B., B. M. Jockusch, R. R. Friis, R. Back, E. Grundmann, and H. Bauer. 1981. Early changes in the distribution and organization of microfilament proteins during cell transformation. *Cell.* 24:175–184.
6. Botstein, D., and R. Maurer. 1982. Genetic approaches to the analysis of microbial development. *Annu. Rev. Genet.* 16:61–83.
7. Byers, B. 1981. Multiple roles of the spindle pole bodies in the life cycle of *Saccharomyces cerevisiae*. *In* Molecular Genetics in Yeast. Alfred Benzon Symposium, 16. D. van Wettstein, J. Friis, M. Kielland-Brandt, and A. Stenderup, editors. Munksgaard, Copenhagen. 119–131.
8. Byers, B. 1981. Cytology of the yeast life cycle. In The Molecular Biology of the Yeast Saccharomyces. J. N. Strathern, E. W. Jones, and J. R. Broach, editors. Cold Spring Harbor Laboratory, Cold Spring Harbor, NY. 1:59–96.
9. Byers, B., and L. Goetsch. 1974. Duplication of spindle plaques and integration of the yeast cell cycle. *Cold Spring Harbor Symp. Quant. Biol.* 38:123–131.
10. Byers, B., and L. Goetsch. 1975. Behaviour of spindles and spindle plaques in the cell cycle and conjugation of *Saccharomyces cerevisiae*. *J. Bacteriol.* 124:511–523.
11. Byers, B., and L. Goetsch. 1976. A highly ordered ring of membrane-associated filaments in budding yeast. *J. Cell Biol.* 69:717–721.
12. Cabib, E., and B. Bowers. 1975. Timing and function of chitin synthesis in yeast. *J. Bacteriol.* 124:1586–1593.
13. Carley, W. W., L. S. Barak, and W. W. Webb. 1981. F-actin aggregates in transformed cells. *J. Cell Biol.* 90:797–802.
14. Chang, M. T., W. F. Dove, and T. G. Laffler. 1983. The periodic synthesis of tubulin in the Physarum cell cycle. Characterization of Physarum tubulins by affinity for monoclonal antibodies and by peptide mapping. *J. Biol. Chem.* 258:1352–1356.
15. Farkaš, V., J. Kovařík, A. Košinova, and Š. Bauer. 1974. Autoradiographic study of mannan incorporation into the growing cell walls of *Saccharomyces cerevisiae*. *J. Bacteriol.* 117:265–269.
16. Faulstich, H., H. Trischmann, and D. Mayer. 1983. Preparation of tetramethylrhodaminyl-phalloidin and uptake of the toxin into short term cultured hepatocytes by endocytosis. *Exp. Cell Res.* 144:73–82.
17. Fisher, P. A., M. Berrios, and G. Blobel. 1982. Isolation and characterization of a proteinaceous subnuclear fraction composed of nuclear matrix, peripheral lamina, and nuclear pore complexes from embryo of *Drosophila melanogaster*. *J. Cell Biol.* 92:674–686.
18. Gallwitz, D. 1982. Construction of a yeast actin gene intron deletion mutant that is defective in splicing and leads to the accumulation of precursor RNA in transformed yeast cells. *Proc. Natl. Acad. Sci. USA.* 79:3493–3497.
19. Gibbons, I. R. 1981. Cilia and flagella of eukaryotes. *J. Cell Biol.* 91(3, Pt. 2):107s–124s.
20. Girbardt, M. 1979. A microfilamentous septal belt (FSB) during induction of cytokinesis in *Trametes versicolor* (L. ex Fr.). *Exp. Mycol.* 3:215–228.
21. Greer, C., and R. Schekman. 1982. Actin from Saccharomyces cerevisiae. *Mol. Cell Biol.* 2:1270–1278.
22. Greer, C., and R. Schekman. 1982. Calcium control of Saccharomyces cerevisiae actin assembly. *Mol. Cell Biol.* 2:1279–1286.

23. Hartwell, L. H. 1967. Macromolecule synthesis in temperature-sensitive mutants of yeast. *J. Bacteriol.* 93:1662–1670.
24. Hayashibe, M., and S. Katohda. 1973. Initiation of budding and chitin ring. *J. Gen. Appl. Microbiol.* 19:23–39.
25. Heath, I. B. 1981. Mitosis through the electron microscope. *In* Mitosis/Cytokinesis. A. M. Zimmerman and A. Forer, editors. Academic Press, Inc., New York. 245–275.
26. Hoch, H. C., and R. J. Howard. 1980. Ultrastructure of freeze-substituted hyphae of the Basidiomycete *Laetisaria arvalis. Protoplasma.* 103:281–297.
27. Hoch, H. C., and R. C. Staples. 1983. Visualisation of actin *in situ* by rhodamine-conjugated phalloin in the fungus *Uromyces phaseoli. Eur. J. Cell Biol.* 32:52–58.
28. Hynes, R. O., and A. T. Destree. 1978. Relationships between fibronectin and actin. *Cell.* 15:875–886.
29. Johnson, G. D., and G. M. de C. Nogueira Araujo. 1981. A simple method of reducing the fading of immunofluorescence during microscopy. *J. Immunol. Meth.* 43:349–350.
30. Kilmartin, J. V. 1981. Purification of yeast tubulin by self-assembly in vitro. *Biochemistry.* 20:3629–3633.
31. Kilmartin, J. V., B. Wright, and C. Milstein. 1982. Rat monoclonal antitubulin antibodies derived by using a new nonsecreting rat cell line. *J. Cell Biol.* 93:576–582.
32. King, S. M., and J. S. Hyams. 1982. The mitotic spindle of *Saccharomyces cerevisiae*: assembly, structure and function. *Micron.* 13:93–117.
33. King, S. M., and J. S. Hyams. 1983. Analysis of anaphase B in *Saccharomyces cerevisiae* using a monoclonal antibody against yeast tubulin. *Eur. J. Cell Biol.* 29:121–125.
34. King, S. M., J. S. Hyams, and A. Luba. 1982. Ultrastructure of mitotic spindles isolated from a cell division cycle mutant of the yeast, *Saccharomyces cerevisiae. Eur. J. Cell Biol.* 28:98–102.
35. King, S. M., J. S. Hyams, and A. Luba. 1982. Absence of microtubule sliding and an analysis of spindle formation and elongation in isolated mitotic spindles from the yeast *Saccharomyces cerevisiae. J. Cell Biol.* 94:341–349.
36. Koteliansky, V. E., M. A. Glukhova, M. V. Bejanian, A. P. Surguchov, and V. N. Smirnow. 1979. Isolation and characterisation of actin-like protein from yeast *Saccharomyces cerevisiae. FEBS (Fed. Eur. Biochem. Soc.) Lett.* 102:55–58.
37. Laemmli, U. K. 1970. Cleavage of structural proteins during the assembly of the head of bacteriophage T4. *Nature (Lond.).* 227:680–685.
38. Lehtonen, E., and R. A. Badley. 1980. Localisation of cytoskeletal proteins in preimplantation mouse embryos. *J. Embryol. Exp. Morphol.* 55:211–225.
39. Lohr, D., R. T. Kovacic, and K. E. Van Holde. 1977. Quantitative analysis of the digestion of yeast chromatin by Staphylococcal nuclease. *Biochemistry.* 16:463–471.
40. McCully, E. K., and C. F. Robinow. 1971. Mitosis in the fission yeast *Schizosaccharomyces pombe*: a comparative study with light and electron microscopy. *J. Cell Sci.* 9:475–507.
41. Moens, P. B., and E. Rapport. 1971. Spindles, spindle plaques, and meiosis in the yeast *Saccharomyces cerevisiae* (Hansen). *J. Cell Biol.* 50:344–361.
42. Neal, M. W., and J. R. Florini. 1973. A rapid method for desalting small volumes of solution. *Anal. Biochem.* 55:328–330.
43. Neff, N. F., J. H. Thomas, P. Grisafi, and D. Botstein. 1983. Isolation of the β-tubulin gene from yeast and demonstration of its essential function in vivo. *Cell.* 33:211–219.
44. Ng, R., and J. Abelson. 1980. Isolation and sequence of the gene for actin in *Saccharomyces cerevisiae. Proc. Natl. Acad. Sci. USA.* 77:3912–3961.
45. Peterson, J. B., R. H. Gray, and H. Ris. 1972. Meiotic spindle plaques in *Saccharomyces cerevisiae. J. Cell Biol.* 53:837–841.
46. Peterson, J. B., and H. Ris. 1976. Electron-microscopic study of the spindle and chromosome movement in the yeast *Saccharomyces cerevisiae. J. Cell Sci.* 22:219–242.
47. Pringle, J. R., and L. H. Hartwell. 1981. The *Saccharomyces cerevisiae* cell cycle. *In* The Molecular Biology of the Yeast Saccharomyces: Life Cycle and Inheritance. J. N. Strathern, E. W. Jones, and J. R. Broach, editors. Cold Spring Harbor Laboratory, Cold Spring Harbor, NY. 97–142.
48. Pringle, J. R., K. Coleman, A. Adams, M. Kelley, R. Longnecker, and P. Oeller. 1982. Cellular morphogenesis in the yeast cell cycle. *J. Cell Biol.* 95(2, Pt. 2):24*a*. (Abstr.)
49. Robinow, C. F., and J. Marak. 1966. A fibre apparatus in the nucleus of the yeast cell. *J. Cell Biol.* 29:129–151.
50. Roth, J., M. Bendayan, E. Carlemalm, W. Villiger, and M. Garavito. 1981. Enhancement of structural preservation and immunocytochemical staining in low temperature embedded pancreatic tissue. *J. Histochem. Cytochem.* 29:663–671.
51. Scherer, S., and R. W. Davis. 1979. Replacement of chromosome segments with altered DNA sequences constructed in vitro. *Proc. Natl. Acad. Sci. USA.* 76:4951–4955.
52. Schroeder, T. E. 1976. Actin in dividing cells: evidence for its role in cleavage but not mitosis. *Cold Spring Harbor Conf. Cell Proliferation.* 3(Book A):265–277.
53. Shortle, D., J. E. Haber, and D. Botstein. 1982. Lethal disruption of the yeast actin gene by integrative DNA transformation. *Science (Wash. DC).* 217:371–373.
54. Sloat, B. F., and J. R. Pringle. 1978. A mutant of yeast defective in cellular morphogenesis. *Science (Wash. DC).* 200:1171–1173.
55. Strathern, J. N., A. J. S. Klar, J. B. Hicks, J. A. Abraham, J. M. Ivy, K. A. Nasmyth, and C. McGill. 1982. Homothallic switching of yeast mating type cassettes is initiated by a double stranded cut in the MAT locus. *Cell.* 31:183–192.
56. Streiblová, E., and M. Girbardt. 1980. Microfilaments and cytoplasmic microtubules in cell division cycle mutants of *Schizosaccharomyces pombe. Can. J. Microbiol.* 26:250–254.
57. Taylor, D. L., and M. Fechheimer. 1982. Cytoplasmic structure and contractility: the solation-contraction coupling hypothesis. *Phil. Trans. R. Soc. Lond. B. Biol. Sci.* B299:185–197.
58. Tkacz, J. S., and J. O. Lampen. 1972. Wall replication in Saccharomyces species: Use of fluorescein-conjugated concanavalin A to reveal the site of mannan insertion. *J. Gen. Microbiol.* 72:243–247.
59. Towbin, H., T. Staehelin, and J. Gordon. 1979. Electrophoretic transfer of proteins from polyacrylamide gels to nitrocellulose sheets: procedure and some applications. *Proc. Natl. Acad. Sci. USA.* 76:4350–4354.
60. Water, R. D., J. R. Pringle, and L. J. Kleinsmith. 1980. Identification of an actin-like protein and of its messenger ribonucleic acid in *Saccharomyces cerevisiae. J. Bacteriol.* 144:1143–1151.
61. Wieland, Th. 1977. Modification of actins by phallotoxins. *Naturwissenschaften.* 64:303–309.
62. Williamson, D. H. 1965. The timing of deoxyribonucleic acid synthesis in the cell cycle of *Saccharomyces cerevisiae. J. Cell Biol.* 25:517–528.
63. Williamson, D. H., and D. J. Fennell. 1975. The use of fluorescent DNA-binding agent for detecting and separating yeast mitochondrial DNA. *Methods* Cell Biol. 12:335–351.
64. Wulf, E., A. Deboben, F. A. Bautz, H. Faulstich, and Th. Wieland. 1979. Fluorescent phallotoxin, a tool for the visualisation of cellular actin. *Proc. Natl. Acad. Sci. USA.* 76:4498–4502.
65. Zechel, K. 1980. Dissociation of the DNase I-actin complex by formamide. *Eur. J. Biochem.* 110:337–341.